Neutrino emissivity from spin-one color superconductors

Andreas Schmitt[*]

Center for Theoretical Physics, Massachusetts Institute of Technology, Cambridge, MA 02139, USA

E-mail: `aschmitt@lns.mit.edu`

Igor A. Shovkovy

Frankfurt Institute for Advanced Studies, J.W. Goethe-Universität, D-60054 Frankfurt am Main, Germany

E-mail: `shovkovy@th.physik.uni-frankfurt.de`

Qun Wang

Department of Modern Physics, University of Science and Technology of China, Hefei, Anhui 230026, People's Republic of China

E-mail: `qunwang@ustc.edu.cn`

We compute neutrino emissivities, specific heat, and the resulting cooling rates in four spin-one color superconductors: color-spin locked, planar, polar, and *A* phases. In particular, the role of anisotropies and point nodes in the quasiparticle excitation spectra are investigated. Furthermore, it is shown that the *A* phase exhibits a helicity order, giving rise to a reflection asymmetry in the neutrino emissivity.

29th Johns Hopkins Workshop on current problems in particle theory: strong matter in the heavens
1-3 August
Budapest

---

[*]Speaker.

---

1. Introduction

The densest matter in nature is expected to exist in neutron stars. The densities in the interior of these compact stellar objects can be of the order of several times the nuclear ground state density. Therefore, the cores of neutron stars are likely to consist of deconfined quark matter [1]. Moreover, the temperature is sufficiently low to allow for color-superconducting states. A color superconductor [2] is characterized by the formation of quark Cooper pairs, analogous to an electromagnetic superconductor, where electrons form Cooper pairs [3]. A multitude of possible color-superconducting phases has been proposed, see e.g., Refs. [4]. Here we consider one-flavor pairing, more precisely, a system of u and d quarks and electrons, where $\langle uu \rangle$ and $\langle dd \rangle$ Cooper pairs are formed. These Cooper pairs carry total spin one [5]. Among all possible spin-one phases, the isotropic color-spin-locked (CSL) phase is the ground state in an isotropic medium without external fields [6]. In a more complicated scenario, however, the ground state is unknown. Here we consider, in addition to the CSL phase, also the planar, polar and A phases [6, 7]. The three latter ones exhibit anisotropic gap functions. In particular, the gap functions in the polar and A phases have nodes at the north and south pole of the Fermi sphere.

2. Neutrino emissivity

We consider the direct Urca processes $u + e^- \to d + \nu$ (electron capture) and $d \to u + e^- + \overline{\nu}$ (β-decay). They provide the most efficient cooling processes of neutron stars [8]. Our starting point to compute the time derivative of the neutrino and antineutrino distribution functions is the kinetic equation, obtained within the Kadanoff-Baym formalism [9, 10]

$$i\partial_X^\lambda \text{Tr}[\gamma_\lambda G_\nu^<(X, P_\nu)] = -\text{Tr}\left[G_\nu^>(X, P_\nu)\Sigma_\nu^<(X, P_\nu) - \Sigma_\nu^>(X, P_\nu)G_\nu^<(X, P_\nu)\right], \quad (2.1)$$

where the trace runs over Dirac space. (Here and in the following, the index ν always labels neutrino quantities and should not be confused with a Lorentz index.) The quantities $G_\nu^{<,>}(X, P_\nu)$ and $\Sigma_\nu^{<,>}(X, P_\nu)$ are the neutrino Green functions and self-energies, both slowly varying functions of the space-time coordinate $X = (t, \mathbf{x})$. The leading order contributions to the neutrino self-energies which enter the kinetic equation (2.1) are given by the diagrams in Fig. 1. For the sake of simplicity, we do not take strange quarks into account. Their weak interactions are Cabibbo suppressed, and their number density is not expected to be very large. (Admittedly, however, the bigger phase space for the Urca processes involving massive strange quarks may partially compensate this suppression.) For the explicit expressions of the functions $G_\nu^{<,>}(X, P_\nu)$ and $\Sigma_\nu^{<,>}(X, P_\nu)$ see Ref. [11]. Also see this reference for the details of the derivation which, starting from Eq. (2.1), leads to the result

$$\frac{\partial}{\partial t} f_\nu(t, \mathbf{p}_\nu) = \frac{\partial}{\partial t} f_{\overline{\nu}}(t, \mathbf{p}_\nu) \simeq -\frac{4\alpha_s G_F^2}{3\pi^4} \mu_e \mu_u \mu_d T^2 \sum_r \int_{-1}^1 d\xi \, (1 - \xi \cos\theta_\nu) F_{\varphi_u \varphi_d}^{rr}(\xi, w). \quad (2.2)$$

where f_ν and $f_{\overline{\nu}}$ are the neutrino and antineutrino distribution functions, respectively. Moreover, α_s is the strong coupling constant, G_F the Fermi coupling constant, T the temperature, and μ_e, μ_u, and μ_d the chemical potentials for electrons, u and d quarks, respectively. The result holds for isotropic phases as well as for phases in which the order parameter picks a special direction in momentum
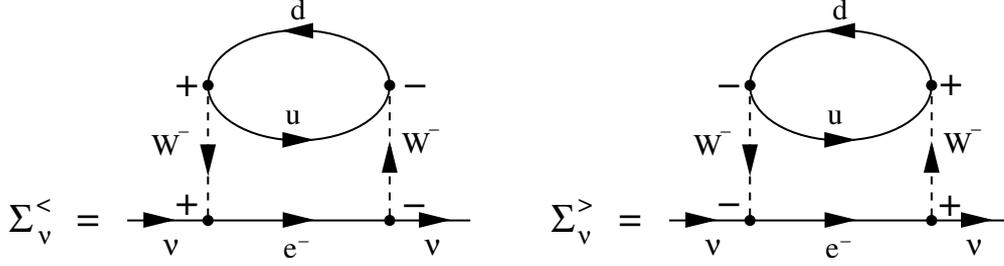
2

Figure 1: Neutrino self-energies relevant for the neutrino Urca processes in the close-time-path formalism. The $+$ and $-$ signs assign the vertices to the upper and lower branch of the time contour, respectively.

Table 1: Angular dependence of the energy gap (functions $\lambda_{\xi,r}$) and the functions $\omega_{rr}(\xi)$ for four spin-one color superconductors.

phase	$\omega_{11}(\xi)$	$\lambda_{\xi,1}$	$\omega_{22}(\xi)$	$\lambda_{\xi,2}$	$\omega_{33}(\xi)$	$\lambda_{\xi,3}$
CSL	2	2	1	0	–	–
planar	2	$1+\xi^2$	1	0	–	–
polar	2	$1-\xi^2$	1	0	–	–
A	$1+\mathrm{sgn}(\xi)$	$(1+|\xi|)^2$	$1-\mathrm{sgn}(\xi)$	$(1-|\xi|)^2$	1	0

space, identified with the z direction. We denote the angle between the neutrino momentum and the z-axis by θ_ν. The function F in the integrand depends on the energy gaps $\phi_{u,d}$ via $\varphi_{u,d} \equiv \phi_{u,d}/T$, on the neutrino momentum p_ν via $w \equiv p_\nu/T$, and on $\xi \equiv \cos\theta_u = \cos\theta_d$ with $\theta_{u,d}$ being the angle between the z-axis and the up (down) quark momentum. Its explicit form is

$$F^{rr}_{\varphi_u \varphi_d}(\xi, w) = \omega_{rr}(\xi) \sum_{e_1, e_2 = \pm} \int_0^\infty \int_0^\infty dx\, dy \left(e^{-e_1 \sqrt{y^2 + \lambda_{\xi,r} \varphi_u^2}} + 1 \right)^{-1} \left(e^{e_2 \sqrt{x^2 + \lambda_{\xi,r} \varphi_d^2}} + 1 \right)^{-1}$$

$$\times \left(e^{w + e_1 \sqrt{y^2 + \lambda_{\xi,r} \varphi_u^2} - e_2 \sqrt{x^2 + \lambda_{\xi,r} \varphi_d^2}} + 1 \right)^{-1} \quad (2.3)$$

The index r labels the different excitation branches in the respective spin-one color superconductor. In general, the quasiparticle excitation is given by

$$\varepsilon_{\mathbf{k},r,f} = \sqrt{(k - \mu_f)^2 + \lambda_{\xi,r} \phi_f^2} \,, \quad (2.4)$$

where $f = u, d$ and $\xi = \cos\theta_{\mathbf{k}}$, $\theta_{\mathbf{k}}$ being the angle between the z-axis and the quark momentum. The functions $\omega_{rr}(\xi)$ and $\lambda_{\xi,r}$ are different for each phase. In Table 1 we list these quantities for the four spin-one color-superconducting phases considered here. From Eq. (2.2), it is straightforward to compute the neutrino emissivity

$$\varepsilon_\nu \equiv -\frac{\partial}{\partial t} \int \frac{d^3 \mathbf{p}_\nu}{(2\pi)^3} p_\nu \left[f_\nu(t, \mathbf{p}_\nu) + f_{\bar\nu}(t, \mathbf{p}_\nu) \right] = -2 \frac{\partial}{\partial t} \int \frac{d^3 \mathbf{p}_\nu}{(2\pi)^3} p_\nu f_\nu(t, \mathbf{p}_\nu) \,. \quad (2.5)$$

We obtain

$$\varepsilon_\nu = \frac{457}{630} \alpha_s G_F^2 T^6 \mu_e \mu_u \mu_d \left[\frac{1}{3} + \frac{2}{3} G(\varphi_u, \varphi_d) \right] \,, \quad (2.6)$$
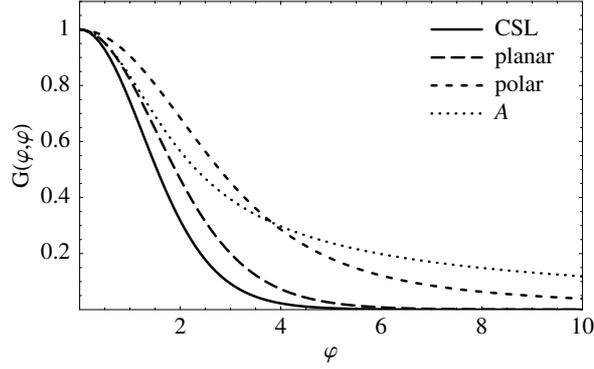
3

Figure 2: Suppression functions $G(\varphi, \varphi)$ of the neutrino emission contributions due to gapped modes in the CSL, planar, polar and A phases.

where

$$G(\varphi_u, \varphi_d) \equiv \frac{1260}{457\pi^6} \int_0^\infty dw\, w^3 \int_{-1}^1 d\xi\, F_{\varphi_u \varphi_d}^{11}(\xi, w) \qquad \text{(CSL, planar, polar)}, \qquad (2.7)$$

$$G(\varphi_u, \varphi_d) \equiv \frac{1260}{457\pi^6} \int_0^\infty dw\, w^3 \int_{-1}^1 d\xi\, \left[F_{\varphi_u \varphi_d}^{11}(\xi, w) + F_{\varphi_u \varphi_d}^{22}(\xi, w) \right] \quad (A). \qquad (2.8)$$

In all phases we consider, the emissivity ε_ν consists of two contributions. The first contribution is given by the term $1/3$ in the square brackets on the right-hand side of Eq. (2.6). It originates from ungapped modes: $r = 2$ in the CSL, planar, and polar phases, and $r = 3$ in the A phase. The second contribution is given by the term proportional to $G(\varphi_u, \varphi_d)$. It originates from the gapped modes. The function $G(\varphi_u, \varphi_d)$ has to be evaluated numerically for each phase separately. For the sake of simplicity, we set $\varphi_u = \varphi_d \equiv \varphi$ in the following. The results for $G(\varphi, \varphi)$ are shown in Fig. 2. The figure shows that the general result in Eqs. (2.6) reproduces the well-known expression for the neutrino emissivity in the normal phase. This is obtained by taking the limit $\varphi \to 0$. Of course, the result in this limit is the same for all considered phases. Since $G(0, 0) = 1$, see Fig. 2, we recover Iwamoto's result [12].

The results for the superconducting phases can be understood from the angular dependence of the respective gap functions, see Table 1. The suppression of the emissivity is largest for the isotropic CSL phase, while nodes in the gap function give rise to the smallest suppression. Analytical calculations for asymptotically large values of φ show an exponential suppression for the CSL and planar phases and a power-law suppression for the polar and A phases [11],

$$G(\varphi, \varphi) \sim \begin{cases} \varphi\, e^{-\sqrt{2}\varphi} & \text{(CSL)}, \\ \sqrt{\varphi}\, e^{-\varphi} & \text{(planar)}, \\ \varphi^{-2} & \text{(polar)}, \\ \varphi^{-1} & (A). \end{cases} \qquad (2.9)$$

It is worth emphasizing that, for small φ, the function $G(\varphi, \varphi)$ cannot be approximated well by the exponential function. For $\varphi \lesssim 1$, the actual suppression is much weaker.

We shall use the results for the emissivity in order to dicuss the effect of spin-one color superconductivity on the cooling of compact stars. This requires also the calculation of the specific heat.
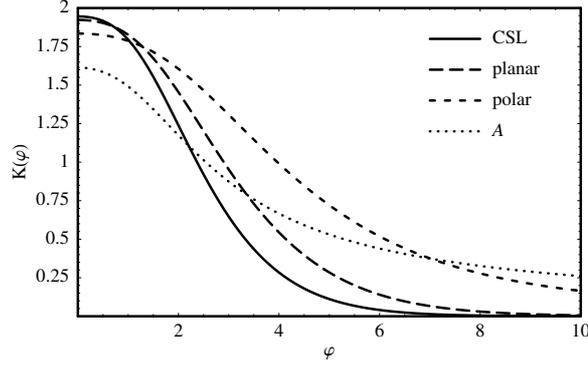
4

Figure 3: The function $K(\varphi)$ for four spin-one color superconductors.

3. Specific heat

The result for the specific heat c_V can be written as [11],

$$c_V = T \sum_{f=u,d} \mu_f^2 \left[\frac{1}{3} + \frac{2}{3} K(\varphi_f) \right] . \tag{3.1}$$

The structure of this result is analogous to that of emissivity in Eq. (2.6), i.e., the first and the second terms in the square brackets on the right-hand side come from ungapped and gapped modes, respectively. The explicit form of the function $K(\varphi)$ reads

$$K(\varphi) = \frac{3}{\pi^2} \int_0^\infty dx \int_{-1}^1 d\xi \frac{e^{\sqrt{x^2+\lambda_{\xi,1}\varphi^2}}}{\left(e^{\sqrt{x^2+\lambda_{\xi,1}\varphi^2}}+1\right)^2} \left[x^2 + \lambda_{\xi,1}\left(\varphi^2 + \frac{\phi_0^2}{T_c^2}\right)\right]$$

$$\text{(CSL, planar, polar),} \tag{3.2}$$

$$K(\varphi) = \frac{3}{2\pi^2} \sum_{r=1}^2 \int_0^\infty dx \int_{-1}^1 d\xi \frac{e^{\sqrt{x^2+\lambda_{\xi,r}\varphi^2}}}{\left(e^{\sqrt{x^2+\lambda_{\xi,r}\varphi^2}}+1\right)^2} \left[x^2 + \lambda_{\xi,r}\left(\varphi^2 + \frac{\phi_0^2}{T_c^2}\right)\right] \quad (A). \tag{3.3}$$

Here, ϕ_0 is the value of the energy gap at zero temperature, and T_c is the critical temperature for the superconducting phase transition. The numerical results for the function $K(\varphi)$ for all considered cases are shown in Fig. 3. The different values of the function for different phases at $\varphi = 0$ indicate the jump of the specific heat at the second order phase transition. As for the emissivities, one may derive analytical approximate expressions for the specific heat at asymptotically large φ, corresponding to asymptotically small temperatures [11],

$$K(\varphi) \sim \begin{cases} \varphi^{5/2} e^{-\sqrt{2}\varphi} & \text{(CSL)}, \\ \varphi^2 e^{-\varphi} & \text{(planar)}, \\ \varphi^{-2} & \text{(polar)}, \\ \varphi^{-1} & \text{(A)}. \end{cases} \tag{3.4}$$

Again, both phases without nodes of the gap function exhibit an exponential behavior, while the phases with point nodes at the north and south pole of the Fermi sphere behave according to a power-law.

5

4. Cooling rates

In order to study cooling of bulk matter in spin-one color-superconducting phases, we assume the neutrino emissivity to be the only source of energy loss. Then

$$\varepsilon_\nu(T) = -c_V(T)\frac{dT}{dt},$$

(4.1)

Integrating this equation yields

$$t - t_0 = -\int_{T_0}^{T} dT' \frac{c_V(T')}{\varepsilon_\nu(T')},$$

(4.2)

where T_0 is the temperature at time t_0. By inserting the expressions from Eqs. (2.6) and (3.1) into Eq. (4.2) and using $\varphi_u = \varphi_d \equiv \varphi$, we derive

$$t - t_0 = -\frac{630}{457}\frac{\mu_u^2 + \mu_d^2}{\alpha_s G_F^2 \mu_e \mu_u \mu_d}\int_{T_0}^{T}\frac{dT'}{(T')^5}\frac{1 + 2K(T')}{1 + 2G(T')},$$

(4.3)

where the temperature-dependent functions $K(T)$ and $G(T)$ are obtained from the functions $K(\varphi)$ and $G(\varphi, \varphi)$ with the help of the model temperature dependence of the energy gap,

$$\phi_f(T) = \phi_0\sqrt{1 - (T/T_c)^2}.$$

(4.4)

By making use of Eq. (4.3), let us estimate the cooling behavior of a compact star whose core is made out of spin-one color-superconducting quark matter. We start from the moment when the stellar core, to a good approximation, becomes isothermal. At this point, the stellar age is of the order of $t_0 = 10^2$ yr and the temperature is about $T_0 = 100$ keV. The estimates in the literature [13, 14] suggest that the value of the critical temperature in spin-one color superconductors is of the order of $T_c = 50$ keV. This is the value that we use in the numerical analysis. Moreover, we choose $\mu_u = 400$ MeV, $\mu_d = 500$ MeV, $\mu_e = 100$ MeV, $\alpha_s = 1$. The Fermi weak coupling constant is given by $G_F = 1.16637 \times 10^{-11}$ MeV^{-2}.

The numerical results show that the cooling behavior is dominated by the ungapped modes. Consequently, to a very good approximation, the time dependence of the temperature can be computed by neglecting the functions $K(T')$ and $G(T')$ in Eq. (4.3). In this case, an analytical expression can be easily derived,

$$T(t) = \frac{T_0\,\tau^{1/4}}{(t - t_0 + \tau)^{1/4}},$$

(4.5)

where

$$\tau \equiv \frac{315}{914}\frac{\mu_u^2 + \mu_d^2}{\alpha_s G_F^2 \mu_e \mu_u \mu_d}\frac{1}{T_0^4}.$$

(4.6)

With the above parameters, this constant is of the order of several minutes, $\tau \simeq 10^{-5}$yr.

It may be interesting, although unphysical, to compare the cooling behavior of the gapped modes of the different spin-one phases. To this end, we drop the 1 in the numerator and denominator of the integrand in Eq. (4.3). The results are shown in Fig. 4. Note that both the initial temperature T_0 and the critical temperature T_c are beyond the scale of the figure. The reason is that, even for the gapped modes, the cooling time scale for temperatures down to approximately 10 keV is
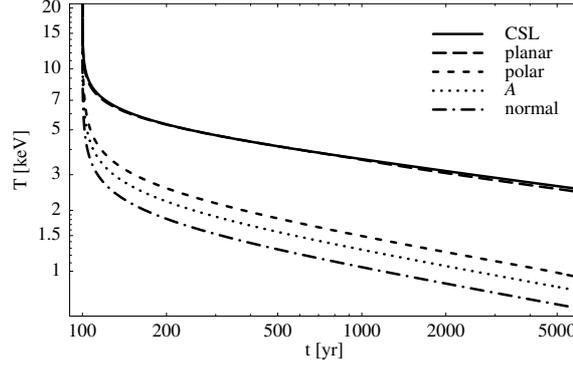
6

Figure 4: Temperature as a function of time for normal quark matter and four spin-one "toy phases" (dropping the fully ungapped modes).

set by the above constant τ. Therefore, all phases cool down very fast, and the transition to the superconducting phase at $T = 50$ keV is hidden in the almost vertical shape of the curve. Only at temperatures several times smaller than T_c, i.e., of the order of 10 keV, substantial differences between the phases appear. In this range, the fully gapped phases cool down considerably slower than the phases with nodes on the Fermi sphere, which, in turn, cool slower than the normal phase. It seems to agree with physical intuition that this order reflects the order of the suppression at low temperatures for the neutrino emissivity, i.e., the slowest cooling (isotropic gap) happens for the phase where ε_ν is suppressed strongest while the fastest cooling (no gap) happens for the smallest suppression. Note, however, that the cooling depends on the ratio of the suppressions of ε_ν and c_V. Therefore, this order is a nontrivial consequence of the exact forms of the functions $G(\varphi, \varphi)$ and $K(\varphi)$. For large values of φ, we may use Eqs. (2.9) and (3.4) to estimate the ratio $K(\varphi)/G(\varphi, \varphi)$. For both completely gapped phases we find $K(\varphi)/G(\varphi, \varphi) \sim \varphi^{3/2}$ while both phases with point nodes yield ratios independent of φ. Consequently, for late times, $T \sim t^{-2/11}$ in the CSL and planar phases while $T \sim t^{-1/4}$ in the polar, A and normal phases.

5. Spatial asymmetry in the neutrino emission from the A phase

In this section, we address a special aspect of the angular distribution of the neutrino emission. To this end, we consider the net momentum carried away by neutrinos and antineutrinos from the quark system per unit volume and time,

$$\frac{d\mathbf{P}^{(net)}}{dV\,dt} \equiv -\frac{\partial}{\partial t}\int\frac{d^3\mathbf{p}_\nu}{(2\pi)^3}\,\mathbf{p}_\nu\,[f_\nu(t,\mathbf{p}_\nu) + f_{\overline{\nu}}(t,\mathbf{p}_\nu)] = -2\frac{\partial}{\partial t}\int\frac{d^3\mathbf{p}_\nu}{(2\pi)^3}\,\mathbf{p}_\nu\,f_\nu(t,\mathbf{p}_\nu). \quad (5.1)$$

Analogously to the case of the total emissivity, see Eq. (2.6), we arrive at the following general result,

$$\frac{d\mathbf{P}^{(net)}}{dV\,dt} = \frac{457}{945}\alpha_s G_F^2 T^6 \mu_e\mu_u\mu_d\,H(\varphi_u, \varphi_d)\,\hat{\mathbf{z}}\,, \quad (5.2)$$

where $\hat{\mathbf{z}}$ is the unit vector in z direction, and

$$H(\varphi_u, \varphi_d) \equiv -\frac{420}{457\pi^6}\int_0^\infty dw\,w^3\int_{-1}^1 d\xi\,\xi\,F^{11}_{\varphi_u\varphi_d}(\xi, w) = 0 \quad \text{(CSL, planar, polar)}, \quad (5.3)$$

$$H(\varphi_u, \varphi_d) \equiv -\frac{420}{457\pi^6}\int_0^\infty dw\,w^3\int_{-1}^1 d\xi\,\xi\,\left[F^{11}_{\varphi_u\varphi_d}(\xi, w) + F^{22}_{\varphi_u\varphi_d}(\xi, w)\right] \quad (A). \quad (5.4)$$
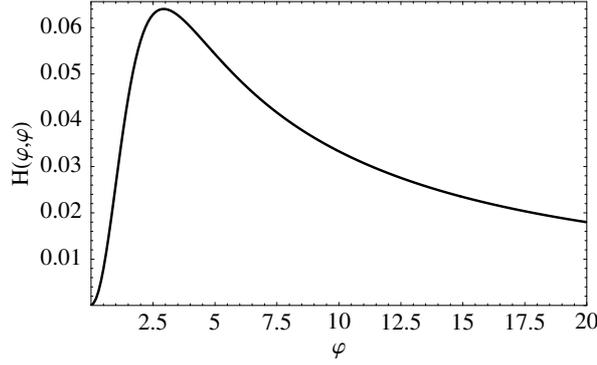
7

Figure 5: Numerical results for the function $H(\varphi, \varphi)$ which determine the net momentum carried away from the spin-1 color superconducting A phase by neutrinos.

In the CSL, planar, and polar phases, the function $H(\varphi_u, \varphi_d)$ is identically zero. This is because $F^{11}_{\varphi_u \varphi_d}(\xi, w)$ is an even function of ξ in these three phases, and therefore the integration over ξ in Eq. (5.3) is vanishing. This means that the net momentum of emitted neutrinos as well as the related net recoil momentum of bulk quark matter in the CSL, planar, and polar phases are zero.

The result is non-vanishing, however, in the A phase. The corresponding function $H(\varphi, \varphi)$ is plotted in Fig. 5. From the figure, we see that $H(0,0) = 0$. Of course, this is just a consistency check that, in the limit $\varphi \to 0$, we reproduce the vanishing result in the fully isotropic normal phase of quark matter. From the numerical data, we find that the maximum value of the function $H(\varphi, \varphi)$ is approximately equal to 0.064, which corresponds to the value of its argument $\varphi \simeq 2.9$. At large φ, the asymptotic behavior of $H(\varphi, \varphi)$ is power suppressed as $1/\varphi$.

It may look surprising that the net momentum from the A phase is nonzero, indicating an asymmetry in the neutrino emission with respect to the reflection of the z-axis. The gap functions do not exhibit this asymmetry.

The origin of this remarkable result can be made transparent by rewriting the expression (5.4) for the A phase in the following way,

$$H(\varphi_u, \varphi_d) = -\frac{840}{457\pi^6} \int_0^\infty dw\, w^3 \int_{-1}^1 d\xi\, \xi\, F^{\text{eff}}_{\varphi_u \varphi_d}(\xi, w), \tag{5.5}$$

where

$$F^{\text{eff}}_{\varphi_u \varphi_d}(\xi, w) \equiv \sum_{e_1, e_2 = \pm} \int_0^\infty \int_0^\infty dx\, dy \left(e^{-e_1 \sqrt{y^2 + (1+\xi)^2 \varphi_u^2}} + 1\right)^{-1} \left(e^{e_2 \sqrt{x^2 + (1+\xi)^2 \varphi_d^2}} + 1\right)^{-1}$$

$$\times \left(e^{w + e_1 \sqrt{y^2 + (1+\xi)^2 \varphi_u^2} - e_2 \sqrt{x^2 + (1+\xi)^2 \varphi_d^2}} + 1\right)^{-1}. \tag{5.6}$$

In the derivation, we used the explicit forms of $\omega_{rr}(\xi)$ and $\lambda_{\xi, r}$ from Table 1. Now, the result looks as if only one single quasiparticle mode contributes to the net neutrino momentum. The corresponding "effective" gap function has the angular dependence $\sim (1 + \xi)$ which clearly discriminates between $+z$ and $-z$ directions.

In order to understand the physical reason for the appearance of the effective quasiparticle mode, it is useful to analyze the physical properties of the gapped modes of the A phase, $r = 1, 2$.
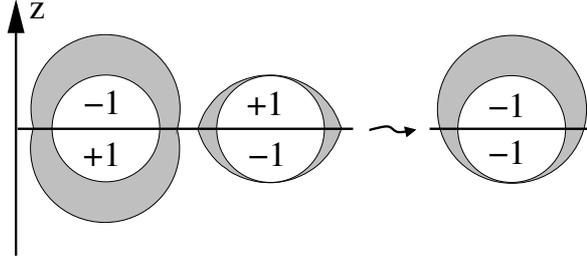
Figure 6: Gap functions for the first (left) and the second (middle) excitation branch with specified helicities of quasiparticles in the upper and the lower hemispheres. The "effective" gap relevant for the neutrino emission is shown on the right.

The color-spin structure of these modes is encoded in the projection operators $\mathscr{P}^+_{\mathbf{k},r}$, which project onto a subspace in color-spin space corresponding to the r-th quasiparticle. These projectors appear in the quark propagators [6]. It is instructive to write the first two projectors in the form

$$\mathscr{P}^+_{\mathbf{k},1} = \frac{1}{2}J_3^2[1 - \mathrm{sgn}(\hat{k}_3)]H^+(\hat{\mathbf{k}}) + \frac{1}{2}J_3^2[1 + \mathrm{sgn}(\hat{k}_3)]H^-(\hat{\mathbf{k}}) , \qquad (5.7)$$

$$\mathscr{P}^+_{\mathbf{k},2} = \frac{1}{2}J_3^2[1 + \mathrm{sgn}(\hat{k}_3)]H^+(\hat{\mathbf{k}}) + \frac{1}{2}J_3^2[1 - \mathrm{sgn}(\hat{k}_3)]H^-(\hat{\mathbf{k}}) , \qquad (5.8)$$

where $J_3^2 = \mathrm{diag}(1,1,0)$ is a matrix in color space (indicating that quarks of the third color are unpaired), and $H^\pm(\hat{\mathbf{k}}) \equiv \frac{1}{2}(1 \pm \Sigma \cdot \hat{\mathbf{k}})$ are the helicity projectors with $\Sigma \equiv \gamma^5\gamma^0\gamma$. From Eq. (5.7) we see that the quasiparticles of the first branch have helicity $+1$ when the projection of their momentum onto the z-axis is negative, $\hat{k}_3 < 0$, and helicity -1 if $\hat{k}_3 > 0$. Quasiparticles of the second branch have opposite helicities, see Eq. (5.8).

The next step in the argument is to notice that only left-handed quarks participate in the weak interactions which underly the Urca processes. In the ultrarelativistic limit, these are quarks with negative helicity. Taking into account the helicity properties of the quasiparticles in the *A* phase, it becomes clear that only an effective gap structure contributes. This is constructed from the upper hemisphere of the first mode and the lower hemisphere of the second mode, see Fig. 6. This is a graphical representation of the formal argument given after Eq. (5.6). [Of course, our choice for the angular dependence of the gap functions, namely $\lambda_{\mathbf{k},1} = (1 + |\cos\theta_\mathbf{k}|)^2$ and $\lambda_{\mathbf{k},2} = (1 - |\cos\theta_\mathbf{k}|)^2$, is only one possible convention. Equivalently, one could choose $\lambda_{\mathbf{k},1} = (1 + \cos\theta_\mathbf{k})^2$ and $\lambda_{\mathbf{k},2} = (1 - \cos\theta_\mathbf{k})^2$, in which case the quasiparticle excitations would be ordered according to their helicity. Then, quasiparticles of the first (second) branch would have negative (positive) helicity, and the weak interaction would involve only quasiparticles of the first branch. Our convention in this paper is in accordance with Ref. [6].]

The asymmetry in the effective gap function translates into the asymmetry of the neutrino emission. This is due to the angular dependence of the amplitude for Urca type processes. As in the vacuum, the corresponding amplitude squared is proportional to $1 - \cos\theta_{vd}$, where θ_{vd} is the angle between the neutrino and down quark momenta. Such an angular dependence of the amplitude means that the neutrinos are preferably emitted in the direction opposite to the (almost collinear) momenta of the participating up and down quarks. In fact, this is a general property that

9

holds also in the normal phase [12]. Since the effective gap function assumes smaller values for quasiparticles with $\hat{k}_3 < 0$ than with $\hat{k}_3 > 0$, there is more neutrino emission in the $+z$ direction.

One can estimate the maximum velocity of a neutron star with a quark matter core in the A phase that can be obtained by the asymmetric neutrino emission. It has been shown that this velocity is negligibly small, e.g., of the order 1 m/s, see erratum in Ref. [15]. In essence, the reason for this is that the available thermal energy in the star, after matter in the stellar interior cools down to the critical temperature $T_c \lesssim 100\,\text{keV}$ of the A phase, is too small to power substantial momentum kicks. (It would be interesting to investigate, however, if additional sources of stellar heating, e.g., such as the latent heat from a first-order phase transition, could change the conclusion.)

Acknowledgments

References

[1] J. C. Collins and M. J. Perry, Phys. Rev. Lett. **34**, 1353 (1975).

[2] D. Bailin and A. Love, Phys. Rept. **107**, 325 (1984).

[3] J. Bardeen, L. N. Cooper and J. R. Schrieffer, Phys. Rev. **108**, 1175 (1957).

[4] K. Rajagopal and F. Wilczek, hep-ph/0011333; D. H. Rischke, Prog. Part. Nucl. Phys. **52**, 197 (2004); I. A. Shovkovy, nucl-th/0410091.

[5] M. Iwasaki and T. Iwado, Phys. Lett. B **350**, 163 (1995).

[6] A. Schmitt, Phys. Rev. D **71**, 054016 (2005).

[7] T. Schäfer, Phys. Rev. D **62**, 094007 (2000).

[8] D. G. Yakovlev, A. D. Kaminker, O. Y. Gnedin and P. Haensel, Phys. Rept. **354**, 1 (2001).

[9] L. P. Kadanoff and G. Baym, *Quantum Statistical Mechanics* (Benjamin, New York, 1962).

[10] M. Schönhofen, M. Cubero, B. L. Friman, W. Nörenberg and G. Wolf, Nucl. Phys. A **572**, 112 (1994).

[11] A. Schmitt, I. A. Shovkovy and Q. Wang, hep-ph/0510347.

[12] N. Iwamoto, Phys. Rev. Lett. **44**, 1637 (1980).

[13] W. E. Brown, J. T. Liu and H.-C. Ren, Phys. Rev. D **62**, 054016 (2000).

[14] A. Schmitt, Q. Wang and D. H. Rischke, Phys. Rev. D **66**, 114010 (2002).

[15] A. Schmitt, I. A. Shovkovy and Q. Wang, Phys. Rev. Lett. **94**, 211101 (2005) [Erratum-ibid. **95**, 159902 (2005)].

PoS(JHW2005)028